



Serbian Tribology  
Society

# SERBIATRIB '19

16<sup>th</sup> International Conference on  
Tribology



Faculty of Engineering  
University of Kragujevac

Kragujevac, Serbia, 15 – 17 May 2019

## EXPERIMENTAL STUDY OF $\text{MoS}_2$ COATED GEARS TESTED IN VACUUM AFTER EXPOSURE TO HUMIDITY

Iqbal SHAREEF<sup>1,\*</sup>, Timothy KRANTZ<sup>2</sup>, Zachary CAMERON<sup>2</sup>, Tysen MULDER<sup>2</sup>

<sup>1</sup>Bradley University, Peoria, IL, USA

<sup>2</sup>NASA Glenn Research Center, Cleveland, OH, USA

\*Corresponding author: shareef@bradley.edu

**Abstract:** Space Industry commonly uses molybdenum disulphide ( $\text{MoS}_2$ ) as a solid lubricant film on gears in a variety of mechanisms. These mechanisms are often exposed to humid air during fabrication, integration into higher-level assemblies, and storage. It is generally accepted that operating  $\text{MoS}_2$  films in humid environments has a detrimental effect on the film's lifetime compared to operation in vacuum. However, the effect of exposure of such films to humid air with subsequent operation in vacuum is not well understood. In this study, a sputtered  $\text{MoS}_2$  dry film lubricant coating was applied to steel gears, which were then tested in a vacuum environment. Half of the spur gears coated with  $\text{MoS}_2$  were exposed to approximately 58 percent relative humidity for up to 77 days before testing. The other half set of gears were not exposed to humid air before testing. All gears were tested in a vacuum gear test rig. Gear tooth forces and the radial displacement of the gears were recorded during testing. These data together with photos, videos, Scanning Electron Microscope (SEM) inspections of worn gears, and Energy-Dispersive X-ray (EDX) spectra were analysed. For purposes of this study, the coating durability was defined as the time until the start of the coating degradation as was evident from increase of friction. Assessment of the results obtained from all experiments indicate that gears exposed to humid air prior to operation in vacuum showed nearly 36 percent reduction in coating durability, on average. SEM and EDX analyses of wear debris indicate mainly  $\text{MoS}_2$  was present with minor traces of other elements. The worn surfaces of gears show significant content of  $\text{MoS}_2$  still remaining in the gear teeth's contact area.

**Keywords:** Molybdenum Disulfide, Solid Lubricant, Thin Film, Surface Coating, Spur Gears, Rolling Contact, Mild Wear, Debris Formation.

### 1. INTRODUCTION

The purpose of this work was to study the effect of humid air exposure on the durability of a molybdenum disulfide ( $\text{MoS}_2$ ) dry film lubricant coating on spur gears operated in vacuum. Certain extreme space environments preclude the use of wet lubrication. For such situations,  $\text{MoS}_2$ -based coatings are often used for a wide variety of space mechanisms. Such coatings are typically exposed to humid air environments during integration, ground

operations, and storage prior to launch. It is well known that if a mechanism with a  $\text{MoS}_2$  sputtered coating is operated in humid air instead of vacuum its durability is reduced. However, the practical implications of exposing  $\text{MoS}_2$  coatings to humidity for extended periods of time, and then subsequently operating them in vacuum, are not fully understood.

Lince, Loewenthal, and Clark provide a recent, and thorough, discussion of previous studies regarding  $\text{MoS}_2$  aging and oxidation. They comment that life test data for sputter-

deposited MoS<sub>2</sub> coatings that were held in long-term storage are uncommon [1]. They also completed and reported a study on the degradation of three nanocomposite MoS<sub>2</sub> coatings after storage in humid air. The tests used to evaluate coating endurance were pin-on-disk tests, and storage times were up to 2.3 years. They found that exposure to humid air could degrade the endurance of the coatings by up to 55 percent. The severity of degradation depended on both the duration of exposure and the composition of the coating.

A dedicated study of such effects has not been conducted for MoS<sub>2</sub> coatings on gear teeth. The purpose of this study was to investigate the influence of exposure to humid air on the subsequent durability of a sputtered MoS<sub>2</sub> coating on spur gears. While previous work by others studied nanocomposite MoS<sub>2</sub> coatings [1], the focus of this work was a pure MoS<sub>2</sub> coating.

## 2. EXPERIMENTAL METHODOLOGY

### 2.1 MoS<sub>2</sub> Coated Test gears

Readily available stock gears with the appropriate center distances to fit in the test stand were selected and customized for this study. The customizations of the stock gear design were the bore diameters and the face widths. The pinions and gears were 3mm module spur gears with standard tooth proportions. The pinions had 26 teeth and a 13 mm face width. The gears had 48 teeth and a 10 mm face width. The study used six pairs of pinions and gears made from S45C steel (equivalent to AISI 1045). The teeth were induction hardened to surface hardness of 50-60 HRC, and then finished ground.

All twelve test pinions and gears were coated with sputtered MoS<sub>2</sub>. Because of the sputtering chamber capacity, two coating runs were required. Witness coupons were in the chamber during sputtering. The thickness of the coating on the witness coupons was reported by the vendor to be 37,000 angstroms for the first run and 30,000 angstroms for the second run. After coating, the test gears were sealed in bags using a dry

inert cover gas. Pinions and gears to be tested as unexposed remained in the sealed bags until they were to be installed in the test rig. The time from the opening of the bag, until the gears were in a vacuum condition in the test rig, was minimized to all practical extent.

Prior to sputtering, the tooth surface roughness was measured along the involute profile direction of a randomly selected pinion tooth using a stylus profilometer. An untested coated pinion tooth that had been exposed to humidity was also inspected. The surface roughness data were filtered using an ISO standard Gaussian filter with 0.8 mm cutoff and 300:1 bandwidth. The resulting calculated roughness average value of 0.42 micrometer Ra was the same for both of the profilometer traces. The peak-to-valley range of the filtered roughness data was approximately the same as the measured coating thickness. The roughness topography features were the same prior to and after sputtering as shown in Fig. 1.

One half of the available mating tooth surface pairs were exposed to humid air prior to testing. The exposure was done in a closed chamber with the gears placed on a perforated plate. Beneath the plate was a saturated solution of water and sodium bromide. The saturated salt solution provided a relative humidity of approximately 58 percent, this value being near to the upper limit 60 percent relative humidity of certain storage conditions for the mechanisms of interest.

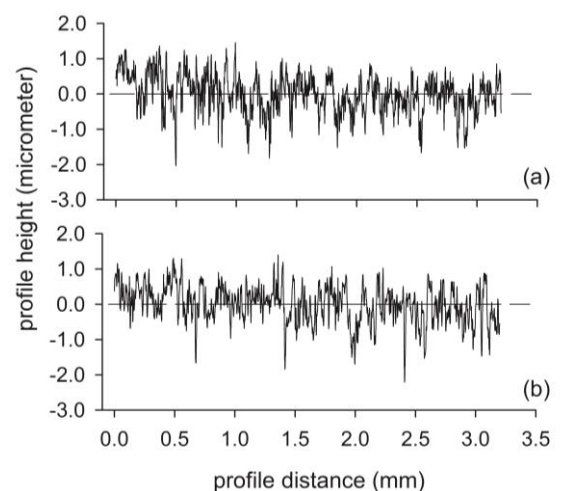


**Figure 1.** Surface roughness profiles along the involute direction of pinion teeth: (a) Prior to sputtering, (b) After sputtering, and exposure to humid air.

## 2.2 Gear Test Rig

To accomplish gear testing, a vacuum test rig, previously used for roller testing [2-4], was adapted for gear testing. To adapt the rig, the spacing from the input to the output shaft was increased from 36 mm to 112 mm. Otherwise, the rig setup was the same as had been used for roller testing.

The vacuum gear rig is depicted as a schematic in Figure 2. The pinion is driven by a variable speed electric motor. A magnetic-particle brake attached to the output shaft imposes torque on the gear. The position of the pinion is controlled by a pressurized air cylinder, which moves the drive motor plate about a pivot point. Increasing the air cylinder's height swings the pinion, in an arc motion, into mesh with the gear. The pressure to the cylinder, and thereby shaft center distance, is adjusted by a hand-operated valve. A linear variable displacement transducer (LVDT) measures the position of the drive motor plate relative to the bedplate the output of which was used to establish the proper operating center distance. The rig turntable, when rotated, provides controlled misalignment of shafts for roller experiments. For gear testing, the turntable was adjusted to provide for an aligned shaft condition. A turbomolecular pump, assisted by a scroll pump, provides vacuum in the test chamber. Ferrofluid seals maintain the vacuum at the shaft-chamber interfaces. The typical condition in the test chamber is a pressure of  $3 \times 10^{-7}$  Torr. The most prevalent remaining constituent in the chamber during testing is water vapor as was determined using a residual gas analyzer.

The torque on the output shaft is measured by a strain-gage type torque meter with a capacity of 22 N-m (200 in-lb). Calibration was done in place using deadweights acting on a torque arm attached at the test gear position and reacted by the output shaft to ground.

The force created by the meshing gear teeth can be described as three orthogonal forces. Each of these force components influences a sensor described with the aid of Figure 2.

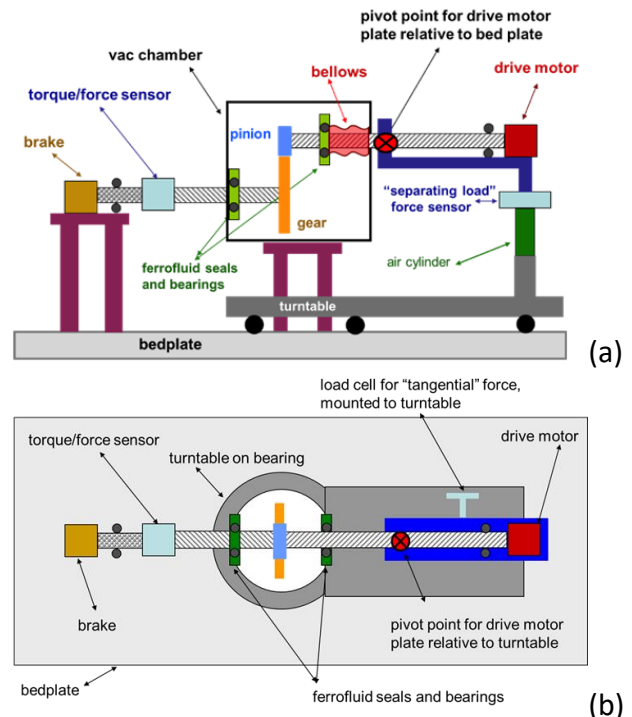


**Figure 2.** Schematic representation of vacuum gear rig: (a) Side view, (b) Overhead view.

The tooth force component directed tangent to the pitch circle is termed the tangential force. The torque on the gear is a product of the tangential force and the operating pitch radius. The gear tooth tangential force attempts to rotate the drive motor plate about a pivot axis, but the table is constrained to the turntable through a load sensor termed as the "tangential" force sensor in Figure 2. The separating force is the tooth force directed along the line joining the gear centers, which acts through a pivot axis and attempts to tilt the drive motor table. This motion is resisted by the air cylinder through a sensor termed the "separating load" force sensor. Because the drive motor plate is not balanced about the pivot point, the force measured on this "separating load" force sensor is a combination of the gear separating force action and the unbalanced overhung weight of the motor and plate. The third component of gear tooth force acts along the axial direction of the gear shaft, the gearing thrust force. The force is measured using a strain-gage type force sensor that is integrated with the torque meter. Although spur gears theoretically create zero thrust forces, in practice a thrust force is created because of

inevitable manufacturing tolerances and small mounting misalignments. The magnitude of the resulting thrust force depends in part on the friction between the mating gear teeth. The action of spur gears creating a thrust force is analogous to the friction-dependent thrust forces created by misaligned rollers [2].

Shaft speeds and total number of shaft revolutions were measured using encoders on each shaft. The encoder pulses were counted and recorded via a digital pulse counter. The encoders provide 6,000 pulses for each shaft revolution.

The LVDT measures the tilting position of the drive motor plate. The tilting of the plate changes the pinion-to-gear center distance, and so the LVDT output thereby measures the operating center distance of the gears. As the gears operate, the operating center distance changes slightly because of the gearing action. As the tooth contact position on the pinion moves from the dedendum, through the pitch point, and then to the addendum region, the friction force changes direction. This changing friction force causes slight changes in the instantaneous center distance, because of elastic deflections, and thereby the friction condition affects the output of the LVDT.

The gear teeth surface conditions were photographed at regular intervals during testing through a viewport. The images were captured using a 12-megapixel digital single-lens reflex camera with a 150 mm micro lens.

## 2.3 Experimental Procedure

The experimental approach was to conduct an equal number of tests using unexposed and exposed surfaces. The test matrix is shown in Table 1. The pinions and gears were assigned randomly as six test pairings per Table 1. With the ability to test front (side "A") and back (side "B") faces of each tooth, 12 tests were possible. Test article pairings 1 through 4 were assigned to have side "A" tested with zero exposure to humid air, except for some minimal exposure time in air during installation of the MoS<sub>2</sub> coated gears into the test rig. For purposes of this study, such

minimal exposure is considered as zero exposure for all analysis purposes. For test article pairings one through four, once sides "A" of the teeth were tested, the pair was placed into the humidity exposure chamber to begin the exposure time for the tooth sides "B". For gear pair five, there was zero exposure to humidity before sides "A" of the teeth was tested. Then the vacuum test rig was opened for minimum amount of time needed to remove the gears from the mounting shafts and immediately reinstall the gears for testing of teeth sides "B" as also unexposed. For test article pair six, the pinion and gear were placed into the humidity exposure chamber at the beginning of the test program to obtain a long exposure time while testing the other gears. Both sides "A" and "B" of pair 6 were tested after an exposure time of 77 days. The exposure times for other test were less than 77 days as was dictated by the testing pace and sequence.

As the test sequence progressed, it was decided that photo documentation of the conditions of the teeth prior to testing might prove insightful. Beginning with the fifth test in the testing order sequence (test MoS<sub>2</sub> 4-A, per Table 1), the first step of the testing sequence was to document the visual condition of each gear with digital photographs. Next, the gear pair was mounted onto the test rig shafts, and then the chamber vacuum condition was established over several hours (typically overnight). The chamber pressure was  $7 \times 10^{-7}$  Torr or less at the beginning of each test. Figure 3 shows a pair of the MoS<sub>2</sub> coated test gears out of sealed bags just prior to test, and in the test chamber just prior to closing the vacuum chamber door for testing.

Testing was done at a constant motor speed, and brake torque. The test speed was 80 rpm for the pinion and consequently 43.3 rpm for the gear. The speed was selected as the maximum speed that did not induce any significant rig dynamic loading or vibrations as had been determined by previous testing of similar test gears. The torque was 6.8 Nm for the gear as applied by the brake and measured

by torque sensor. The power transmitted was 31 watts. The torque was selected to provide tooth load intensity (force per unit face width) similar to the tooth load intensity for the mechanisms of interest. Testing for endurance of the coatings typically required durations longer than a working day, and unattended testing was not desirable. The testing was paused overnight, as needed, with the test chamber vacuum maintained by continuous operation of the turbo-pump. Testing would then be resumed the following day.

The test progression was monitored by visual inspection of the tooth surfaces through a viewport, aided at times by a strobe light to “freeze” the rotating motion of the gears. The visual condition was also recorded by digital photographs illuminated by a short duration flash through a second viewport that provided a view of the gear teeth, but not of pinion teeth. In addition, a video camera was used to continuously record the contacting region of the gear and pinion at all times except during the visual examination with a strobe light.

**Table 1.** Test matrix, naming conventions, and test sequence.

Test Name	Test Article Pairing	Pinion Serial Number	Gear Serial Number	Tooth Side Loaded	Exposed	Total Exposure Time (days)	Testing Order Sequence
MOS <sub>2</sub> 1-A	1	P4	G1	A	No	-	1
MOS <sub>2</sub> 1-B				B	Yes	10	3
MOS <sub>2</sub> 2-A	2	P6	G6	A	No	-	2
MOS <sub>2</sub> 2-B				B	Yes	28	6
MOS <sub>2</sub> 3-A	3	P2	G2	A	No	-	4
MOS <sub>2</sub> 3-B				B	Yes	17	9
MOS <sub>2</sub> 4-A	4	P1	G3	A	No	-	5
MOS <sub>2</sub> 4-B				B	Yes	17	10
MOS <sub>2</sub> 5-A	5	P3	G5	A	No	-	7
MOS <sub>2</sub> 5-B				B	No	-	8
MOS <sub>2</sub> 6-A	6	P5	G4	A	Yes	77	11
MOS <sub>2</sub> 6-B				B	Yes	77	12



(a)



(b)

**Figure 3.** Test gears: (a) Just prior to testing, (b) Installed in rig just prior to closing test chamber.

The test progression was monitored by displays of the sensor data plotted as functions of pinion revolutions. Previous developmental tests revealed that as wear severity and friction of the MoS<sub>2</sub> coating increased, sensor outputs became more erratic even though their mean value remains nearly same. For example, when friction of the gear teeth increases, the range of the instantaneous separation force increases even though the mean value over time may still be the same. This phenomenon is the result of the tooth friction force reversing direction as the tooth contact passes through the pitch point. Thereby, the friction force first adds to, and then subtracts from, the magnitude of the separating force during the tooth mesh cycle. With higher tooth friction the excursions from the mean value becomes larger. These observations and experience in health monitoring of geared machines led to the definition and use of “condition indicators” as a means to monitor the overall capability of the MoS<sub>2</sub> films to provide low friction.

Condition indicators were defined as follows. Data records were collected for 1 second at 1 kHz sampling rate. For each second of data recorded, the standard deviation was calculated as the “condition indicator”, stored, and plotted as a function of accumulated pinion revolutions. Such condition indicators proved to be reliable indicators of a change in the MoS<sub>2</sub> coating’s performance. Figure 4(a) provides a trend plot from test MoS<sub>2</sub> 1-B of the condition indicator for the LVDT sensor that measures gear center distance changes. Marked on the plot is the indication where the MoS<sub>2</sub> began to become compromised. Also marked are three regions: Region I being the break-in and smooth running regime, Region II where the MoS<sub>2</sub> first showed indication of being compromised, and Region III being a significant friction regime. An example of raw recorded data, from which a “condition indicator” was calculated, is shown in Figure 4(b) for the thrust force sensor during operation in Region III. In plot of 4(b) there was relatively high tooth friction during the last 400 samples of this particular data record causing a varying thrust force.

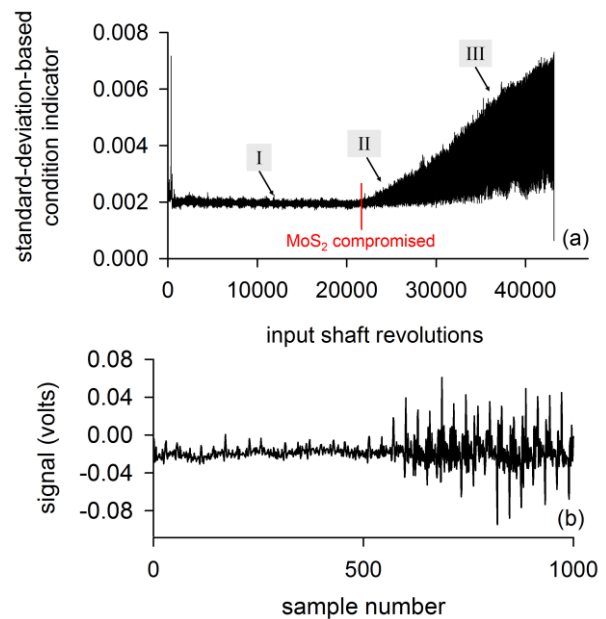


**Figure 4.** Typical trend and features of a condition indicator of MoS<sub>2</sub> film function: (a) Trend of condition indicator for the center distance (LVDT sensor) for test 1-B, (b) Typical data record for calculation of standard-deviation-based condition indicator.

Film durability was determined using the condition indicator trend plots. The film durability was defined as the number of pinion revolutions until the film compromise started, as indicated on Figure 4. The film compromise was defined as the very beginning of progressive degradation of the film’s performance. A mechanism may continue to perform its intended function for some time after such film degradation begins. For this study defining the durability as the beginning of performance degradation provided a useful comparison of the film durability with and without exposure to humid air.

### 3. RESULTS

The results of quantitative measures of film durability will be discussed first. As described in the previous section, “condition indicators” were calculated from sensor data. A condition indicator value was calculated every second for each force and displacement sensor monitored. Figure 4(a) is an example of condition indicator data trend plot from the test 1-B. The number of pinion revolutions corresponding to the start of film compromise,

as marked on Figure 4, was determined for each test by visual inspection of such trend plots. The film's durability measure was determined from three sensors: the gear center distance, the gear thrust force, and the gear tangent force sensors. For each test, film durability was calculated as the average of the cycles till compromised indicator from each of the three sensors. The results are shown in Table 2.

**Table 2.** Test Results of Film Durability.

Test Name	Exposure (days)	Film Durability (pinion revolutions)			
		Center Distance	Thrust Force	Tangent Force	Average Value *
MOS2 1-A	0	52,000	52,000	56,000	53,333
MOS2 2-A	0	59,000	61,000	65,000	61,667
MOS2 3-A	0	207,000	184,000	180,000	190,333
MOS2 4-A	0	86,000	69,000	94,000	83,000
MOS2 5-A	0	125,000	125,000	136,000	128,667
MOS2 5-B	0	83,000	80,000	89,000	84,000
MOS2 1-B	10	21,000	20,000	22,000	21,000
MOS2 2-B	28	69,000	55,000	74,000	66,000
MOS2 3-B	17	59,000	65,000	66,000	63,333
MOS2 4-B	17	81,000	78,000	95,000	84,667
MOS2 6-A	77	84,000	76,000	88,000	82,667
MOS2 6-B	77	70,000	71,000	74,000	71,667

\* average value is the average of the 3 columns to the left

unexposed group	average = 100,200	median = 83,500
exposed group	average = 64,900	median = 68,800
percent reduction	35%	18%

As can be seen from Table 2, on average the film durability was shorter for gears exposed to humid air compared to gears with zero exposure. The film durability for gears with zero exposure ranged from 53,300 to 190,300 pinion revolutions with an average value of 100,200 and a median value of 83,500 revolutions. The film durability for gears exposed to humid air ranged from 21,000 to 84,700 pinion revolutions with an average value of 64,900 and a median value of 68,800 revolutions. Using the unexposed-gear film durability as a baseline, the exposure reduced the film durability by 35 percent based on average values or 18 percent based on median values. These reductions in film durability are similar in magnitude compared to the 55 to 20 percent range of reductions reported by Lince, Loewenthal, and Clark [1].

The film durability values, from the "Average Value" column of Table 2, are plotted as a function of the duration of exposure to humid air in Figure 5. The plot shows that while as a group the durability was longest for zero days of exposure, there is no

clear trend of rate of reduction with exposure time. The range of scatter of the film durability for six tests at zero time of exposure is greater than the difference between average durability of exposed and unexposed gears.

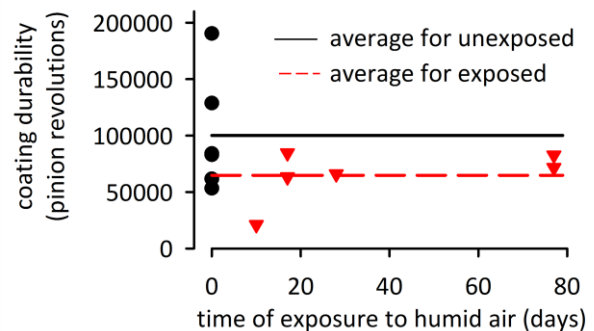


**Figure 5.** Film durability as function of time of exposure to humid air.

The wear of the MoS<sub>2</sub> films was also evaluated with high-resolution optical microphotographs, profilometry scans of the tooth faces, and SEM inspections. During initial running of each gear pair, it was observed that it required very few tooth meshing cycles for the MoS<sub>2</sub> coating's appearance to change. The tooth surface's appearance became glossier and more reflective after only a few revolutions. However, subsequent further visual changes to the tooth surfaces occurred at a very slow and steady rate. Figure 6 illustrates typical results of how the gear surface's visual appearance changed during a test. The first image from left to right shows the teeth prior to any running. The second image was taken after only 1 percent of the total test duration. The other two images of Figure 6 show the teeth after 50 percent and 99 percent of the test duration. These images indicate little change in gear tooth appearance in comparison to the change depicted in the initial 1 percent of the test.

Wear, and running in of pinion teeth were assessed using a stylus profilometer. The teeth were inspected moving the stylus with a 2- $\mu$ m radius conisphere tip across the face width. Because the mating gear tooth face width was slightly less than that of the pinion, there were regions of the pinion tooth near each edge that did not experience contact with the gear.

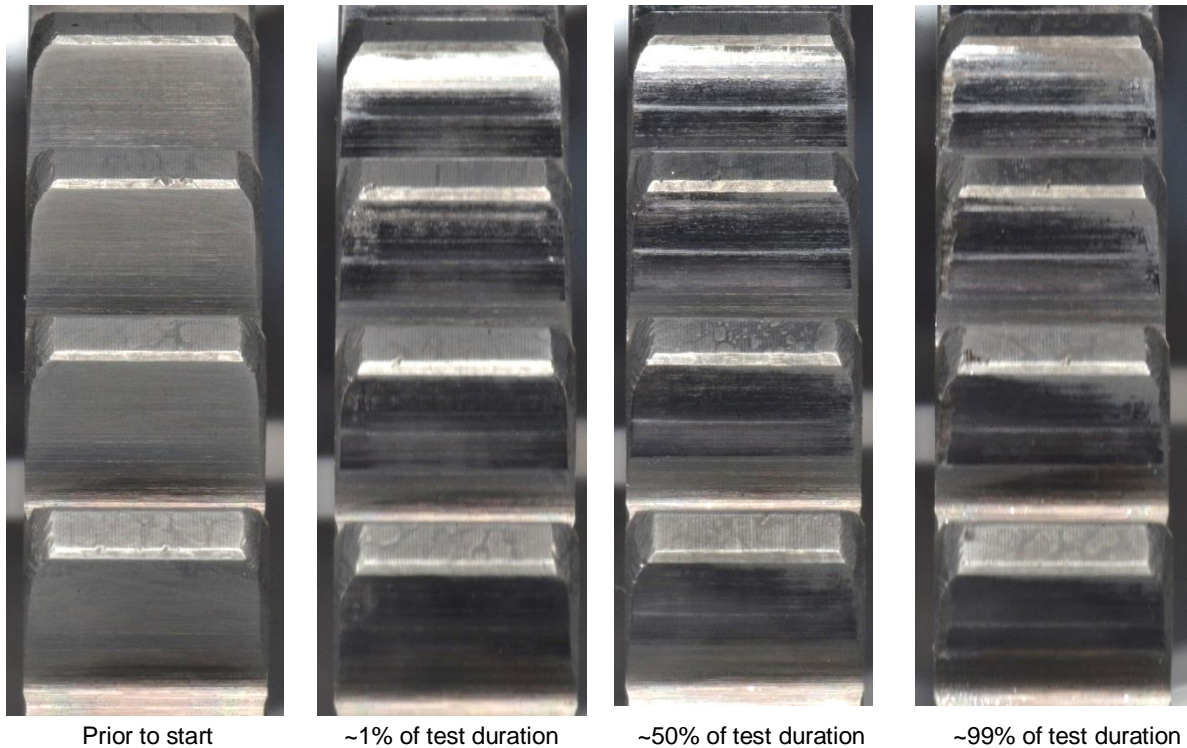


**Figure 6.** Gear teeth surface appearance for different durations of testing.

The data were processed to remove a least-squares linear form, using only the small regions from each edge of the trace that did not experience contact to accomplish the form removal. Traces of teeth prior to test were collected and processed in the same manner. Typical results of the inspections are provided in Figure 7. The data plots of Figures 7(a) and 7(b) is for teeth prior to test. The surfaces show some waviness and some peak and valley features, with peak to valley distances on order of 3 micrometers. The data plots of Figures 7(c) and 7(d) are for tested teeth, and there is an overall wear depth of about 2 micrometers, of which there are some worn regions that are very smooth.

After 77 days of exposure to humid air, small areas of reddish-brown coloration were noted on some teeth of gear set 6. Figure 8 is an example of the noted red-brownish colored spots seen on gear teeth testing in Test 6-A before testing. Close study of digital photographs of the pinions and gears recorded prior to testing revealed that similar spots appeared as early as 17 days after exposure to humidity. However, not all teeth exposed to humidity had colored spots that could be detected. For the pinion and gear pair exposed

for 77 days, there were more red-brownish spots on the gear than there were on the pinion.

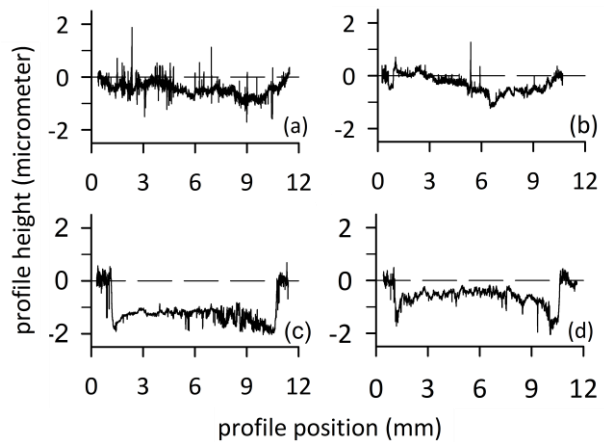


**Figure 7.** Profilometer inspections of pinion teeth with traces along the face width direction: (a) & (b) Prior to test, and (c) & (d) After test.

Teeth with noticeable spots were inspected using a scanning electron microscope (SEM). SEM images were taken at six increasing levels of magnification, and are provided in Figure 9. The image orientation has the gear tooth face width direction in the vertical direction. The vertical lines are topography resulting from grinding of the teeth. This region inspected by SEM revealed that the colored areas included raised material above the surrounding surface.



The highest magnification image reveals details suggesting a “growth” pushing aside and/or through the film.

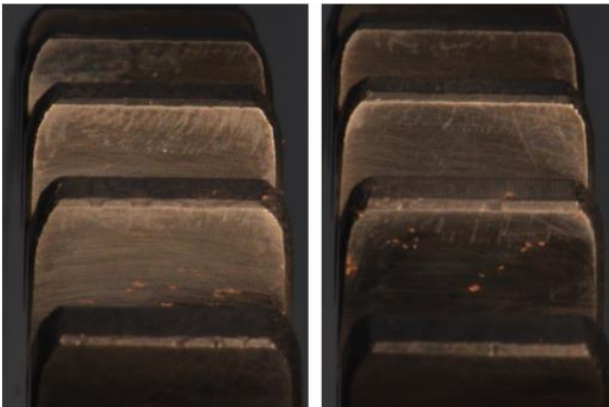


**Figure 8.** Red-brown coloration noted after 77 days exposure to humid air from Test 6-A Gears.

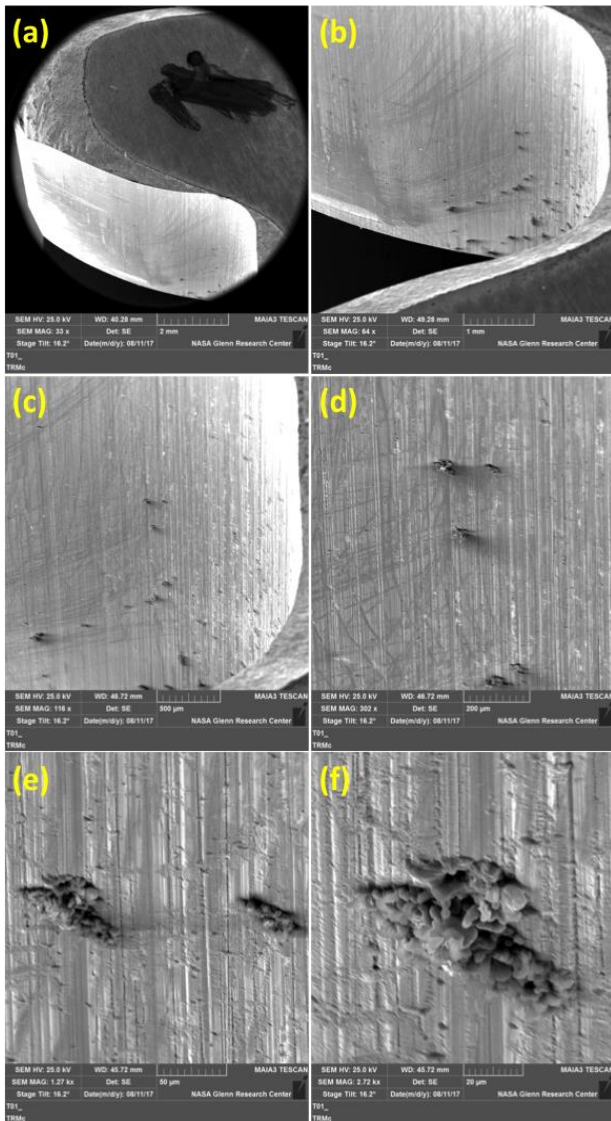
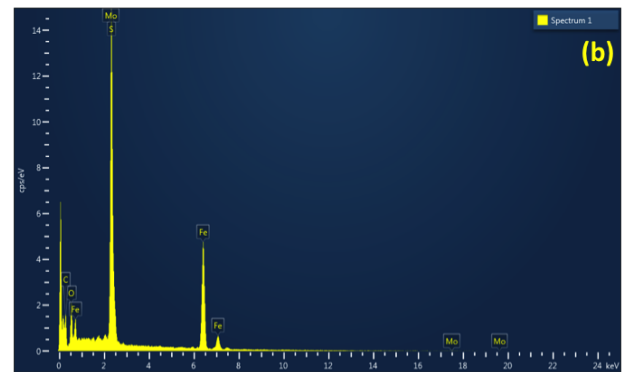
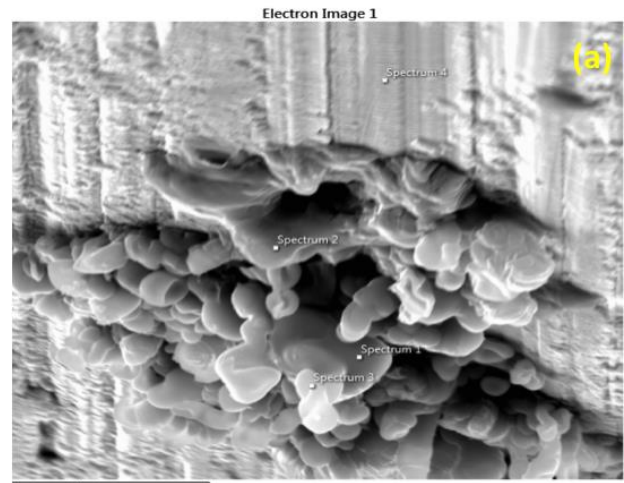


**Figure 9.** SEM Photos of a region having red-brown coloration at six increasing levels of magnification from Test 6-A pinion. The vertical direction is the tooth’s face width direction.



Spectrum Label	Spectrum 1	Spectrum 2	Spectrum 3	Spectrum 4
C	36.83	35	36.07	32.53
O	24.63	24.82	25.84	22.7
Si		0.3		
S	10.09	10.39	9.98	10.58
Mn			0.17	0.24
Fe	14.27	13.86	12.31	16.53
Ni		0.28	0.28	
Mo	14.19	15.35	15.34	17.41
Total	100	100	100	100

Statistics	C	O	Si	S	Mn	Fe	Ni	Mo
Max	36.83	25.84	0.3	10.58	0.24	16.53	0.28	17.41
Min	32.53	22.7	0.3	9.98	0.17	12.31	0.28	14.19
Average	35.11	24.5		10.26		14.24		15.57
Std. Dev	1.87	1.31		0.28		1.74		1.34

**Figure 10.** SEM inspection using energy-dispersive spectroscopy: (a) Regions inspected, per markings, (b) Spectrum #1 of 4 taken from region 1, typical of all four inspections.

Figure 10(a) provides another SEM image of a similar structure as that of Figure 9(f), from a slightly different viewpoint. During this inspection, energy-dispersive spectroscopy (EDX) was done at the four locations as marked by rectangular regions on Fig. 10(a). The resulting spectrum of Fig. 10(b) is typical of all four inspections. The most prominent peak of the spectrum is associated with Mo (molybdenum), and S (Sulphur). The second prominent peak is associated with Fe (iron). It

is speculated that iron oxidation was occurring at the MoS<sub>2</sub> film-substrate interface and progressed to eventually become evident at the surface.

Study of profilometry data of teeth, prior to test, revealed an inspection with an interesting topography that suggests a fortuitous tracing over a region such as revealed in the SEM images of Figures 9(b) and 10(a). The profilometry data of this inspection, plotted using three different aspect ratios, are provided in Figure 11. The inspection was of pinion P5, in the face width direction, tooth side “B” that later was subjected to test MoS<sub>2</sub> 6-B per Table 1. Figure 11(a) reveals a localized valley feature of about 1.5-micrometer depth but having a prominent peak feature rising above, out of the valley, by about 6 micrometer. Figure 11(b) plotted using an aspect ratio of 20:1 shows some details of the shape of the feature, while Figure 11(c) illustrates the shape with true aspect ratio. The breadth of this feature is about 1.5 micrometer.

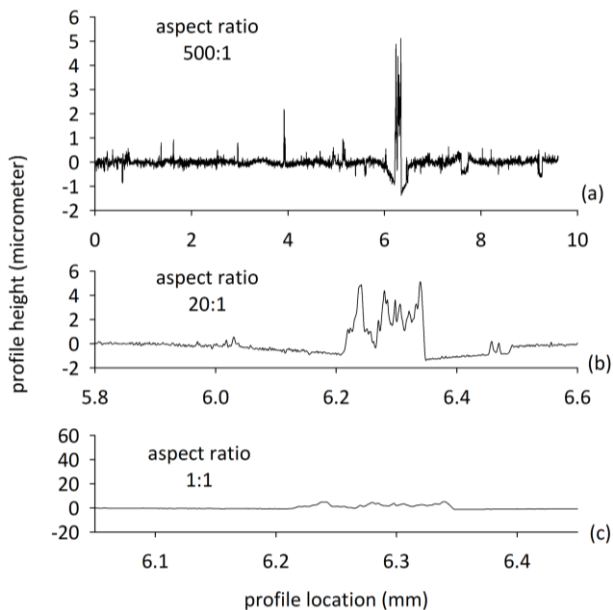


**Figure 11.** Profilometer inspection of a tooth after exposure to humidity for 77 days, prior to test. The same data are plotted using three aspect ratios: 500:1, 20:1, and 1:1.

SEM inspection of a pinion gear tooth, after test 2-A, which was conducted without exposure per Table 1, revealed a wide variety of features on the worn tooth surface. An inspection summary is provided in Figure 12. Figure 12(a) is an optical microscope photo of

the Tooth #1 of the pinion used in Test 2-A, which shows the location of the SEM photomicrographs taken. Figures 12 (b-f) shows a series of SEM photomicrographs of increasing magnification. Figures 12(a) can be used to locate the features of Figures 12(b-c) showing highly smoothed MoS<sub>2</sub>. As the magnification increases in Figure 12(d) slight blistering can be seen around highly smoothed MoS<sub>2</sub>, and with further increase in magnification in Figure 12(e) a region of loss of film thickness is seen, thereby revealing the underlying grinding-line striation topography.

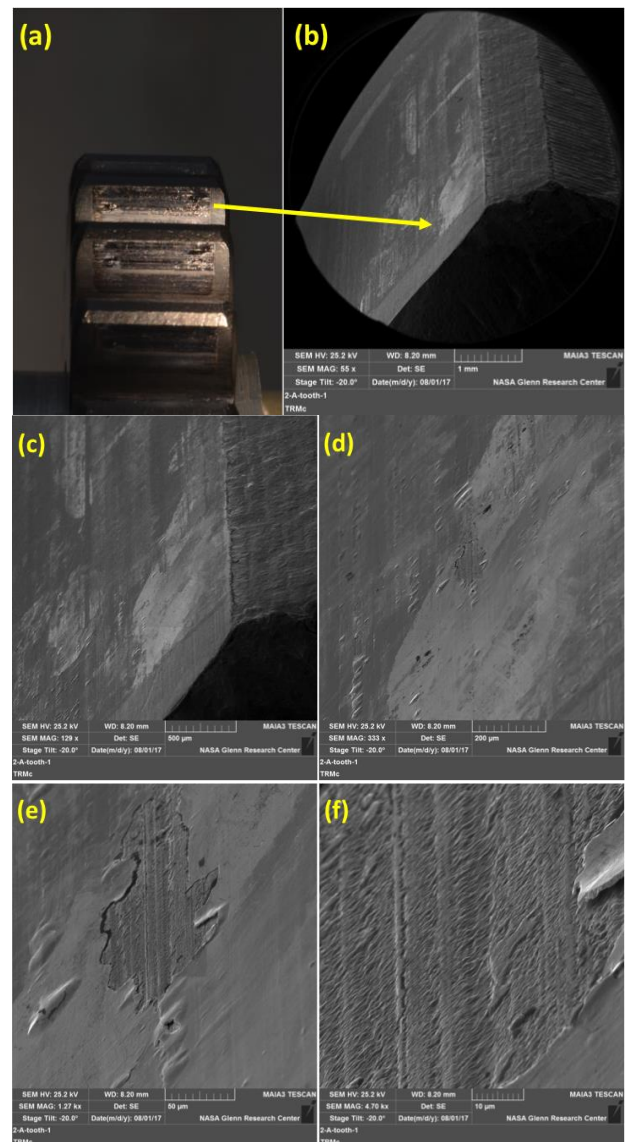


**Figure 12.** Optical and SEM inspection summary of a pinion tooth #1 after test 2A with no exposure to humidity prior to testing: (a) Optical image showing location of SEM inspection, (b) & (c) SEM image of smooth regions of MoS<sub>2</sub> near tooth tip, (d) SEM image of blistering and delamination of the film, (e) & (f) Close up of delaminated region.

The elongated blister features are aligned with the direction of rolling and sliding. Although the “delaminated” region of Fig. 12(e) might suggest exposure of the steel substrate, the higher magnified image of 12(f) has appearance of material flowing in the direction of rolling and sliding.

To investigate the underlying material, an EDX examination of the surface near the center of this region was done at Spectrum location 17 shown in Figure 13(a), and the corresponding Spectrum is shown in Figure 13(b). The result of EDX examination in Figure 13(b) shows spectrum associated with

Molybdenum (Mo), Sulfur (S), and Iron (Fe), thus showing that the region did not experience a complete loss of all MoS<sub>2</sub> through this region. To compare the region below the MoS<sub>2</sub> coating with respect to the MoS<sub>2</sub> coating itself, another EDX examination was done at Spectrum location 18 shown in Figure 13(a), and the corresponding Spectrum is shown in Figure 13(c). A careful examination of the Spectrum 17 and 18 indicate no statistical difference between the underlying region below MoS<sub>2</sub> coating, and the amount of Molybdenum and Sulfur in MoS<sub>2</sub> coating itself.

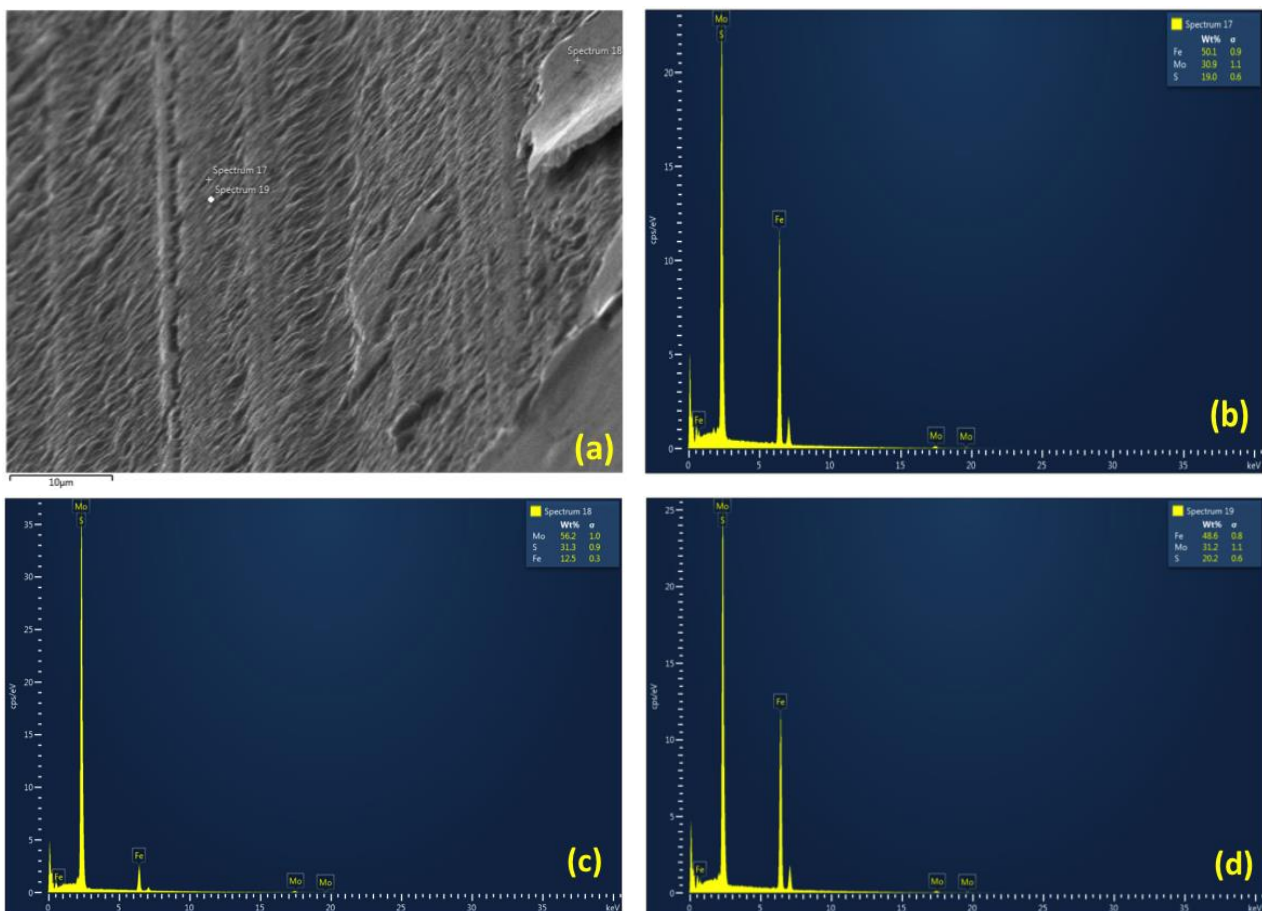


**Figure 13.** EDX examination of the underlying surface below MoS<sub>2</sub> layer: (a) three locations where Spectrum was taken, (b) & (d) spectrums taken from the center of the image, and (c) taken near the right edge.

To double-check the results of the EDX examination of Spectrum 17, another EDX examination was done next to Spectrum 17 location. The location of this EDX probe is shown in Figure 13(a), and the corresponding Spectrum 19 is shown in Figure 13(c) together with a table of Mo, S, Fe weight percentages for all three Spectrums. Comparing the two Spectrums 17 and 19 in the underlying region below MoS<sub>2</sub> coating with the Spectrum 18 of MoS<sub>2</sub> coating itself, it is clear that the underlying region still has significant amount of MoS<sub>2</sub> even after the delamination of the coating layers from the surface.

#### 4. SUMMARY

The purpose of this work was to study the effect of exposure to humid air on the durability of a molybdenum disulfide (MoS<sub>2</sub>) dry film lubricant applied to test spur gears, and subsequently tested in a vacuum environment. MoS<sub>2</sub> was applied by sputtering onto gears made from induction hardened and ground S45C steel. Twelve gear tests were completed in a vacuum gear rig at constant speed and torque. For this study, film durability was defined as the initiation of compromise of the MoS<sub>2</sub>'s ability to provide low friction. Test durations were long enough to initiate this compromise. One-half of the gears tested had zero exposure time to humid air prior to testing. The other half set of the gears were exposed to air of 58 percent relative humidity for exposure durations up to 77 days prior to testing.

On average the film durability time was shorter for gears exposed to humid air compared to gears with zero exposure. The film durability for gears with zero exposure ranged from 190,300 to 53,300 pinion revolutions with an average value of 100,200 and a median value of 83,500 revolutions. The film durability for gears exposed to humid air ranged from 84,700 to 21,000 pinion revolutions with an average value of 64,900 and a median value of 68,800 revolutions. Using the unexposed-gear film durability as a baseline, the exposure reduced the film

durability by 35 percent based on average values or 18 percent based on median values. These reductions in film durability are similar in magnitude to the 55 percent to 20 percent range of reductions reported by Lince, Loewenthal, and Clark [1].

The gear teeth had a very glossy appearance after very few revolutions of the gears. After this initial running in, further change in the appearance of the teeth was a slow, and steady process. Profilometry revealed that the wear depth at test completion was on the order of the specified MoS<sub>2</sub> film thickness.

Red-brown coloration was noted on some of the teeth that had been exposed to humid air. The colored regions appeared as soon as 17 days after exposure to humid air. SEM inspections showed that at least some of these colored areas included material raised above the surrounding MoS<sub>2</sub> film.

#### ACKNOWLEDGEMENT

The NASA Engineering Safety Center (NESC) supported this research. The NASA GRC Summer Faculty Fellowship Program supported Dr. Iqbal Shareef.

#### REFERENCES

- [1] J. Lince, S. Loewenthal, C. Clark, "Degradation of Sputter-Deposited Nanocomposite MoS<sub>2</sub> Coatings for NIRCams during Storage in Air", Proceedings of the 43rd Aerospace Mechanisms Symposium, (May, 2016) pp. 221-234, NASA/CP-2016-219090.
- [2] T. Krantz, C. DellaCorte, M. Dube, "Experimental Investigation of Forces Produced by Misaligned Steel Rollers." Proceedings of the 40<sup>th</sup> Aerospace Mechanisms Symposium, NASA/CP-2010-216272.
- [3] T. Krantz, I. Shareef, "Wear of Steel and Ti6Al4V Rollers in Vacuum." Proceedings of the 41<sup>st</sup> Aerospace Mechanisms Symposium, NASA/CP-2012-21763.
- [4] C. Dellacorte, T. Krantz, M. Dube, "ISS Solar Array Rotary Joint (SARJ) Bearing Failure and Recovery: Technical and Project Management Lessons Learned", NASA/TP-2011-217116.